Spinless Falicov-Kimball model (annealed binary alloy) from large to small dimensions

J. K. Freericks
Institute for Theoretical Physics, University of California, Santa Barbara, California 93106-4030
(Received 29 July 1992)

The phase diagram for the spinless Falicov-Kimball model on a hypercubic lattice is reexamined in the limits of large and small dimensions (for the half-filled ion case). This model is identical to the thermodynamical problem of an annealed binary alloy with diagonal disorder. The phase diagram for the infinite-dimensional case is remarkably similar to the conjectured phase diagram for the one-dimensional case. The system orders in short-period phases, orders in long-period (possibly incommensurate) phases, or segregates, depending on the interaction strength and the electron concentration. The analysis for this simple model provides hope that recently proposed solutions for other interacting fermion models in infinite dimensions will accurately represent the solutions in two and three dimensions.

I. INTRODUCTION

The Falicov-Kimball model[1] was introduced in 1969 to describe the thermodynamics of metal-insulator transitions in compounds that contained both itinerant and localized quasiparticles. The spinless version of the Falicov-Kimball model is the simplest example of an interacting fermionic system that displays numerous phase transitions. The itinerant quasiparticles are called electrons and the localized (static) quasiparticles are called ions. The Hamiltonian is

$$H=-\frac{t^*}{2\sqrt{d}}\sum_{\langle j,k\rangle}(c_j^\dagger c_k+c_k^\dagger c_j)+U\sum_{j=1}^{N}c_j^\dagger c_j W_j -\mu\sum_{j=1}^{N}c_j^\dagger c_j+E\sum_{j=1}^{N}W_j\ , \tag{1}$$

where the electronic hopping term is summed over all nearest-neighbor pairs $\langle j,k\rangle$ of a hypercubic lattice in d dimensions, $c_j^\dagger$ (c_j) is the creation (destruction) operator for a spinless electron at site j, W_j is a classical variable that assumes the value 1 (0) if site j is occupied by (is not occupied by) an ion, U is the electron-ion on-site Coulomb interaction, μ is the electronic chemical potential, and $(-E)$ is the ionic chemical potential. The hopping integral t^* defines the energy unit and will be chosen to be one (all energies are measured in units of t^*). The thermodynamic limit is taken where the number of lattice sites approaches infinity ($N\rightarrow\infty$) but the electron concentration ($\rho_e=\sum_{j=1}^{N}\langle c_j^\dagger c_j\rangle/N$) and the ion concentration ($\rho_i=\sum_{j=1}^{N}W_j/N$) remain constant. The symmetric case of half-filled ions ($\rho_i=\frac{1}{2}$) is the only case considered in this contribution.

The spinless Falicov-Kimball model has a simple interpretation as a thermodynamic model for an annealed binary alloy. A site occupied by an ion ($W_j=1$) is mapped onto a site occupied by an ion type A, a site not occupied by an ion ($W_j=0$) is mapped onto a site occupied by an ion of type B, and U is mapped onto the difference in interaction energies ($U=U_A-U_B$) for ions of type A and type B. The case of half-filled ions ($\rho_i=\frac{1}{2}$) corresponds to the symmetric 50%-50% binary alloy problem.

The ionic configurations are ensemble averaged to represent an annealed binary alloy. This ensemble averaging is what makes the Falicov-Kimball model a full many-body problem. For example, the ground state is determined by the ionic configuration $\Gamma=\{W_j\}$ that minimizes the electronic energy for fixed ion concentration

$$E(U,\rho_e,\rho_i)\equiv\min\left\{E^\Gamma(U,\rho_e)\,\middle|\,\rho_i=\frac{1}{N}\sum_{j=1}^{N}W_j\right\}, \tag{2}$$

where $E^\Gamma(U,\rho_e)$ is the ground-state energy of the Falicov-Kimball Hamiltonian (1) for the ionic configuration Γ at an interaction strength U and an electron concentration ρ_e. The minimization procedure in (2) determines the equivalence class of the ground-state ion configuration Γ_{gs} as a function of the interaction strength, the electron concentration, and the ion concentration.

The Falicov-Kimball model is interesting because it illustrates the competition between order-disorder phase transitions and phase segregation *driven entirely by electronic interactions.*

Brandt and Schmidt[2] and Kennedy and Lieb[3] have proven that for low enough temperatures[4] the ionic configuration Γ of the fully symmetric case ($\rho_e=\rho_i=\frac{1}{2}$) is always ordered into a two-sublattice (bipartite) configuration with the A ions occupying one sublattice and the B ions occupying the other sublattice (chessboard configuration). Numerical studies[5-7] have shown that the zero-temperature phase diagram appears to be an ordered phase (commensurate or incommensurate) for small interaction strength (and large enough electron concentration), and a segregated phase (for almost all electron concentrations) at large interaction strength. This latter result is called the segregation principle and follows physically from the fact that at large interaction strength the electrons avoid the sites occupied by ions and the ground state is determined entirely by the kinetic energy of the electrons. The kinetic energy is minimized

by placing the electrons in the largest possible "box" corresponding to the ions clustering on one side of the lattice. The segregation principle has recently been rigorously proven[8-10] for the one-dimensional case.

Current interest has focused on the infinite-dimensional model after the observation by Metzner and Vollhardt[11] that the many-body problem becomes local in infinite dimensions [when the hopping integral is scaled as in Eq. (1)]. Brandt and Mielsch[12] have analyzed the infinite-dimensional case determining regions in parameter space where the system undergoes a second-order phase transition from a homogeneous (high-temperature) phase to an ordered (two-sublattice) periodic phase. More recent work has analyzed the infinite-dimensional model on a Bethe lattice,[13,14] the zero-temperature phase diagram,[15] Fermi-liquid behavior in a long-range hopping model,[16] and preliminary results for $1/d$ corrections to the infinite-dimensional model.[17]

The Hamiltonian (1) exhibits two kinds of symmetries—an A-B ion-interchange symmetry and an electron-hole symmetry.[3] In the first case, one must consider the A-B interchanged ion configuration Γ^* defined by $\{W_j^*\}=\{1-W_j\}$. The ground states for these two configurations are related by

$$E^{\Gamma^*}(U,\rho_e)=E^{\Gamma}(-U,\rho_e)+U\rho_e \ , \tag{3}$$

for all U and ρ_e. In the second case, the unitary transformation $c_j\rightarrow(-1)^{\epsilon_j}c_j$ and $c_j^\dagger\rightarrow(-1)^{\epsilon_j}c_j^\dagger$ [with $\epsilon_j=1(0)$ for $\mathbf{R}_j$ in sublattice one (two)] that changes the sign of the electron operators on one of the two sublattices (of the bipartite lattice) is used to relate electron eigenvalues with interaction U to corresponding hole eigenvalues with interaction $(-U)$ yielding the result

$$E^{\Gamma}(U,\rho_e)=E^{\Gamma}(-U,1-\rho_e)+U\rho_i \ . \tag{4}$$

These two symmetries are used to reduce the parameter space in the calculation of phase diagrams.

This contribution reanalyzes the one-dimensional solutions[5] and the infinite-dimensional solutions[12] in order to study the qualitative behavior of the spinless Falicov-Kimball model as a function of dimension. Surprisingly, the zero-temperature phase diagrams for both dimensional limits are remarkably similar displaying ordered phases for small interaction strength and segregation for large interaction strength. The model appears to have regions where the periodic phases are described by a label that varies both continuously and discontinuously with the electron concentration. Section II introduces the Green's-function techniques that are employed to solve the model exactly in both limits. Section III discusses the infinite-dimensional case and Sec. IV briefly summarizes the one-dimensional case. Conclusions and conjectures are presented in Sec. V.

II. GREEN'S-FUNCTION TECHNIQUES

The spinless Falicov-Kimball model may be solved exactly in both infinite dimensions and one dimension by determining the local Green's function defined by the matrix element

$$G_{jj}(\omega)\equiv\left\langle j\left|\frac{1}{(\omega-H)}\right|j\right\rangle \ . \tag{5}$$

It is sometimes convenient to write the local Green's function in terms of a (momentum-dependent) self-energy Σ

$$\begin{aligned} G_{jj}(\omega)&=\sum_{\mathbf{k}}G(\mathbf{k},\omega) \ , \\ &=\sum_{\mathbf{k}}[\omega+\mu-\epsilon(\mathbf{k})-\Sigma(\mathbf{k},\omega)]^{-1} \ , \end{aligned} \tag{6}$$

where $\epsilon(\mathbf{k})=-\sum_{j=1}^{d}\cos(\mathbf{k}_j)/\sqrt{d}$ is the band structure of a hypercubic lattice in d dimensions and the momentum summation extends over the entire Brillouin zone.

In infinite dimensions the hopping from one lattice site to another is scaled to zero [see Eq. (1)]. Naively one expects all physical properties to become completely local (and trivial) in this limit. However, the hopping integral is scaled to zero in such a fashion that electrons (virtually) hop from one site to another while the self-energy for the interacting single-particle Green's function remains site diagonal, has no momentum dependence, and is a functional of the local Green's function.[11,12] The many-body problem is solved by mapping onto an auxiliary atomic problem in a time-dependent field (that mimics the hopping of an electron onto a site at a time τ and off the site at a time τ'). The effective action[16,18] for this atomic problem is

$$\begin{aligned} S_{\rm eff}=&\int_0^\beta d\tau\int_0^\beta d\tau' c^\dagger(\tau)G_0^{-1}(\tau-\tau')c(\tau') \\ &+EW+U\int_0^\beta d\tau\, c^\dagger(\tau)c(\tau)W \ , \end{aligned} \tag{7}$$

with W the local ion-occupation number and G_0 the "bare" Green's function that contains *all of the dynamical information of the other sites in the lattice.* The interacting Green's function is determined by

$$G_n^{-1}\equiv G^{-1}(i\omega_n)=G_0^{-1}(i\omega_n)-\Sigma(i\omega_n) \ , \tag{8}$$

at each Matsubara frequency $\omega_n=(2n+1)\pi T$. Since the effective action (7) is quadratic in the electronic variables, the time-dependent atomic problem can be solved for arbitrary bare Green's function G_0 and Eq. (8) employed to determine the functional form of the self-energy in terms of the Green's function.[12] The result is

$$\begin{aligned} \Sigma_n[G]=&\frac{U}{2}-\frac{1}{2G_n}\{1-\mathrm{sgn}(|\omega_n|-\omega_c) \\ &\times\sqrt{1-2(1-2\rho_i[G])UG_n+U^2G_n^2}\}, \end{aligned} \tag{9}$$

with the functional that determines the ionic concentration being

$$\rho_i[G]=\left[1+e^{\beta(E+U/2)}\prod_{n=-\infty}^{\infty}\{1-UG_0(i\omega_n)\}^{-1}\right]^{-1} . \tag{10}$$

The critical frequency ω_c is defined to be the frequency at which the full Green's function becomes pure imaginary

[$\mathrm{Re}G(i\omega_c)=0$]. In this contribution, the energy level E in Eq. (10) is adjusted so that $\rho_i[G]=\frac{1}{2}$.

Note that this representation for the self-energy (9) is formally identical to the coherent-potential approximation[19] with the exception that the dependence of the ion concentration on the electronic Green's functions is explicitly known (for more details on the comparison with the coherent-potential approximation, see Ref. 17). It is this crucial difference that allows for the correct evaluation of the derivatives of the self-energy with respect to the Green's function and produces an exact solution to the annealed binary alloy problem in infinite dimensions.[12] Put in other words, the coherent-potential approximation is exact for all single-particle properties, but not for two-particle properties.

The Green's function is now determined by the self-consistent equation (6). Converting the momentum summation into an integral over energy (since the self-energy has no momentum dependence) yields

$$G_n=F_\infty(i\omega_n+\mu-\Sigma_n[G]) , \tag{11}$$

with $F_\infty(z)$ the scaled complimentary error function of a complex argument[18]

$$\begin{aligned} F_\infty(z)&=\frac{1}{\sqrt{\pi}}\int_{-\infty}^{\infty}dy\frac{e^{-y^2}}{z-y} \\ &=-i\,\mathrm{sgn}[\mathrm{Im}(z)]\sqrt{\pi}e^{-z^2} \\ &\quad\times\mathrm{erfc}\{-i\,\mathrm{sgn}[\mathrm{Im}(z)]z\} . \end{aligned} \tag{12}$$

The self-consistent equation (11) can be tested for solutions that are pure imaginary. In this fashion an equation for the critical frequency[20] is determined:

$$\sqrt{U^2-4\mu^{*2}}F_\infty\left[i\omega_c+\frac{i}{2}\sqrt{U^2-4\mu^{*2}}\right]=1 ,$$

$$\mu^*\equiv\mu-\frac{U}{2} . \tag{13}$$

Note that the critical frequency ω_c vanishes unless U is large enough and it approaches $\sqrt{U^2-4\mu^{*2}}/2$ in the strong-interaction-strength limit ($U\to\infty$).

The electron concentration ρ_e is a monotonic function of the reduced chemical potential μ^* for every temperature T. In the limit as T approaches zero, the electron concentration satisfies

$$\begin{aligned} \rho_e(T\to0,\mu^*)&=\tfrac{1}{2}[1+\theta(\mu^*-U/2)-\theta(-\mu^*-U/2)] \\ &\quad+\frac{1}{\pi}\int_0^\infty d\omega\,\mathrm{Re}\left[G(i\omega)-\frac{i\omega+\mu^*}{(i\omega+\mu^*)^2-\frac{U^2}{4}}\right] , \end{aligned} \tag{14}$$

with $\theta(z)$ the unit step function. When the reduced chemical potential vanishes ($\mu^*=0$), the electronic "band" is half filled ($\rho_e=\frac{1}{2}$); negative values of μ^* correspond to electron concentrations of less than one-half.

The Green's functions can now be employed to study the infinite-dimensional Falicov-Kimball model in the high-temperature (disordered) regime. As the temperature is lowered, a second-order phase transition occurs when the susceptibility for a charge-density-wave distortion diverges. Both the transition temperature and the symmetry of the ordered phase can be determined in the finite-temperature formalism (see Sec. III for details).

In one dimension the zero-temperature Green's functions are determined by the renormalized perturbation expansion[21] in real space,

$$G_{jj}^{-1}(\omega)=\omega+\mu-\Sigma_{jj}(\omega) . \tag{15}$$

The local self-energy is expressed in terms of two continued fractions,

$$\begin{aligned} &\Sigma_{jj}(\omega)=UW_j+\Delta^+(\omega)+\Delta^-(\omega) , \\ &\Delta^\pm(\omega)=\cfrac{1}{\omega-UW_{j\pm1}-\cfrac{1}{\omega-UW_{j\pm2}-\cfrac{1}{\omega-UW_{j\pm3}-\cdots}}} \end{aligned} \tag{16}$$

that depend on the ion occupations (on the line) that lie to the right or to the left of site j. The electronic density of states $n^\Gamma(\omega)$ (for a given ion configuration Γ) is then determined by

$$n^\Gamma(\omega)\equiv-\frac{1}{\pi}\mathrm{Im}\lim_{\epsilon\to0}G(\omega+i\epsilon) , \tag{17}$$

and the electron concentration and internal energy are respectively given by

$$\rho_e=\int_{-\infty}^{\mu}n^\Gamma(\omega)d\omega , \quad E^\Gamma(U,\rho_e)=\int_{-\infty}^{\mu}n^\Gamma(\omega)\omega\,d\omega . \tag{18}$$

The ground-state energy is determined by comparing the internal energy for each ion configuration Γ to determine the minimum energy (ground-state) configuration Γ_{gs} as a function of electron concentration and interaction strength (see Sec. IV for details).

III. THE INFINITE-DIMENSIONAL CASE

At high temperatures the electrons and the ions are uniformly distributed throughout the lattice for all electron concentrations—there is no long-range order. As the temperature is lowered, the homogeneous (disordered) phase becomes unstable to an ordered phase where both the electronic charge density $\sum_j\exp(i\mathbf{q}\cdot\mathbf{R}_j)\langle c_j^\dagger c_j\rangle$ and the A-ion occupation $\sum_j\exp(i\mathbf{q}\cdot\mathbf{R}_j)W_j$ acquire nonzero values (when modulated by the ordering vector $\mathbf{q}$). If this transition is assumed to be a continuous second-order phase transition, then it can be detected when the charge-density-wave susceptibility (at the relevant ordering wave vector) diverges. The static charge-density-wave susceptibility is defined to be the Fourier transform of the electron-electron correlation function

$$\chi(\mathbf{q},T)\equiv-\frac{1}{N}\sum_{\mathbf{R}_j-\mathbf{R}_k}e^{i\mathbf{q}\cdot(\mathbf{R}_j-\mathbf{R}_k)}\times\int_0^\beta d\tau\langle T_\tau c_j^\dagger(\tau)c_j(\tau)\times c_k^\dagger(0)c_k(0)\rangle\ ,$$
$$\equiv T\sum_{n=-\infty}^{\infty}\tilde{\chi}(\mathbf{q},i\omega_n)=T\sum_{n=-\infty}^{\infty}\tilde{\chi}_n(\mathbf{q})\ , \tag{19}$$

for each ordering wave vector $\mathbf{q}$. Dyson's equation[12] is used to relate the full interacting susceptibility $\tilde{\chi}_n$ to the bare susceptibility $\tilde{\chi}_n^0$

$$\tilde{\chi}_n(\mathbf{q})=\tilde{\chi}_n^0(\mathbf{q})-\tilde{\chi}_n^0(\mathbf{q})\sum_{m=-\infty}^{\infty}\frac{\partial\Sigma_n[G]}{\partial G_m}\tilde{\chi}_m(\mathbf{q})\ , \tag{20}$$

with the bare susceptibility defined by[12]

$$\tilde{\chi}_n^0(\mathbf{q})\equiv-\sum_{\mathbf{q}}G_n(\mathbf{k}+\mathbf{q})G_n(\mathbf{k})\ ,$$
$$=-\frac{1}{\sqrt{\pi}}\frac{1}{\sqrt{1-X^2(\mathbf{q})}}\times\int_{-\infty}^{\infty}dy\frac{e^{-y^2}}{i\omega_n+\mu-\Sigma_n-y}\times F_\infty\left[\frac{i\omega_n+\mu-\Sigma_n-X(\mathbf{q})y}{\sqrt{1-X^2(\mathbf{q})}}\right]\ , \tag{21}$$

and all of the wave-vector dependence included in the term $X(\mathbf{q})\equiv\sum_{j=1}^d\cos q_j/d$. The mapping $\mathbf{q}\rightarrow X(\mathbf{q})$ is a many-to-one mapping that determines an equivalence class of wave vectors in the Brillouin zone. "General" wave vectors are all mapped to zero, since $\cos q_j$ can be thought of as a random number between -1 and 1 for general points in the Brillouin zone. Furthermore, all possible values of X ($-1\le X\le 1$) can be labeled by a wave vector that lies on the diagonal of the first Brillouin zone extending from the zone center ($X=1$) to the zone corner ($X=-1$).

The ion-ion correlation functions defined by

$$\chi_{\text{ion-ion}}(\mathbf{q},T)\equiv\frac{1}{TN}\sum_{\mathbf{R}_j-\mathbf{R}_k}e^{i\mathbf{q}\cdot(\mathbf{R}_j-\mathbf{R}_k)}W_jW_k \tag{22}$$

diverge at the same temperature [for the same value of $X(\mathbf{q})$] as the electron-electron correlation functions.[12] Therefore, a divergence of the charge-density-wave susceptibility [$\chi(\mathbf{q},T)$ in Eq. (19)] can be used to determine the long-range order of the ions which is labeled by the same parameter X. An ordering at the zone corner [$X=-1$, $\mathbf{Q}=(\pi,\pi,\ldots)$] corresponds to a two-sublattice (chessboard) state with all of the A ions occupying one sublattice [$\exp(i\mathbf{Q}\cdot\mathbf{R}_j)=1$] and all of the B ions occupying the other sublattice [$\exp(i\mathbf{Q}\cdot\mathbf{R}_j)=-1$]. An ordering at the zone center ($X=1$) corresponds to the segregated phase where the A ions cluster together on one half of the lattice ($\mathbf{R}_1\le 0$) and the B ions cluster together on the other half of the lattice ($\mathbf{R}_1\ge 0$). This latter situation corresponds to the case where the A ions are immiscible in the B ions and do not form a solid solution.

The derivatives of the self-energy with respect to the local Green's functions can be directly performed (for details, see Ref. 12). After some tedious algebra, one finds that the susceptibility $\chi(\mathbf{q},T)$ diverges at the temperature $T_c(X)$ that satisfies

$$1=\frac{U^2}{4}\sum_{n=-\infty}^{\infty}\frac{\eta_n(X)}{[(i\omega_n+\mu^*-\lambda_n)^2-(U^2/4)][(i\omega_n+\mu^*-\lambda_n)\{1+2G_n\eta_n(X)\}-\eta_n(X)]}\ ,$$
$$\equiv\frac{U^2}{4}h(T;X) \tag{23}$$

for each value of X. The parameters $\eta_n(X)$ and λ_n in Eq. (23) are defined by

$$\eta_n(X)\equiv-\frac{G_n}{\tilde{\chi}_n^0(X)}-\frac{1}{G_n}\ ,\quad G_0^{-1}(i\omega_n)\equiv i\omega_n+\mu-\lambda_n\ , \tag{24}$$

respectively. There are three values of X where the integral for $\tilde{\chi}_n^0(X)$ in Eq. (21) can be performed analytically:[12] $X=-1$, $X=0$, and $X=1$. The values of $\eta_n(X)$ are easily determined at these three special points,

$$\eta_n(X=-1)=\lambda_n\ ,\quad \eta_n(X=0)=0\ ,$$
$$\eta_n(X=1)=\frac{1}{2\lambda_n}-\frac{1}{G_n}\ . \tag{25}$$

Note, in particular, that the vanishing of η_n for vanishing X implies that the critical temperature is always zero at a general wave vector [$T_c(X=0)=0$].

In the limit as the temperature gets large, $h(T\rightarrow\infty;X)$ approaches zero as the inverse fourth power of the temperature, since every element of the summand [in Eq. (23)] is asymptotically proportional to $1/\omega_n^4$. In the limit of small temperatures, $h(T\rightarrow 0;X)$ diverges as C/T in the weak-coupling limit ($U\rightarrow 0$) arising from the divergence of the summation [in Eq. (23)] in the limit $T\rightarrow 0$. Therefore, a solution to the transcendental equation (23) will always be found if the coefficient C of the low-temperature divergence is positive. Expanding the function $h(T\rightarrow 0;X)$ about the noninteracting limit in a power series in U yields the following form:[12]

$$h(T\rightarrow 0;X)\equiv\frac{C(\mu^*;X)}{T}\ , \tag{26}$$

for the low-temperature behavior as a function of μ^*. The coefficient $C(\mu^*;X)$ goes through zero at a critical value of the reduced chemical potential $\mu_c^*(X)$. Calculation of $C(\mu^*;X)$ is straightforward near the special values

of X, yielding the following behavior:

$$C(\mu^*;X=-1)=-\frac{1}{\sqrt{\pi}}\int_{|\mu^*|}^{\infty}dy\,e^{-y^2}\left[2\mathrm{Re}F_\infty(y)-\frac{1}{y}\right],$$
$$\mu_c^*(X=-1)\approx 0.250\ ;$$
$$C(\mu^*;X\approx 0)=-\frac{4X}{\sqrt{\pi}}\int_{|\mu^*|}^{\infty}dy\,e^{-y^2}[y-y^2\mathrm{Re}F_\infty(y)]\ ,$$
$$\mu_c^*(X\approx 0)\approx 0.534\ ; \quad (27)$$
$$C(\mu^*;X=1)=\frac{2}{\sqrt{\pi}}\int_{|\mu^*|}^{\infty}dy\,e^{-y^2}[y-\mathrm{Re}F_\infty(y)]\ ,$$
$$\mu_c^*(X=1)\approx 0.613\ .$$

Or, expressed in other words, in the limit as $U\to 0$ solutions to the equation for the critical temperature (23) exist for the chessboard phase ($X=-1$) in the range $0.36\le\rho_e\le 0.64$; for the segregated phase ($X=1$) in the range $0.0\le\rho_e\le 0.19$ and $0.81\le\rho_e\le 1.0$; and for the limit $X\to 0^-(0^+)$ in the range $0.22\le\rho_e\le 0.78$ ($0.0\le\rho_e\le 0.22$ and $0.78\le\rho_e\le 1.0$).

Since all of the wave-vector dependence of $\chi(\mathbf{q},T)$ is included in the scalar $X(\mathbf{q})$, one can study the divergence of $\chi(X,T)$ to determine the equivalence-class label X of the wave vector of the first broken-symmetry phase into which the system has a phase transition. One must examine the critical temperature as a function of X and determine at what value of X the critical temperature is a maximum (the critical temperature for all other values of X is not physically relevant because the susceptibility must be studied from the broken-symmetry phase to see if any additional phase transitions occur as the temperature is lowered below the maximum transition temperature). The value of $X=X_{\max}$ where $T_c(X)$ is a maximum can lie at the boundaries $X=\pm 1$ or someplace in between. If $X_{\max}$ does not lie on the boundary, then the derivative of $T_c(X)$ with respect to X will vanish at $X_{\max}$. The derivative can be calculated by differentiating Eq. (23) with respect to X and using the chain rule. The result is

$$\frac{dT_c(X)}{dX}=-\left[\frac{dh(T;X)}{dT}\right]^{-1}\sum_{n=-\infty}^{\infty}\frac{\eta_n'(X)(i\omega_n+\mu^*-\lambda_n)}{[(i\omega_n+\mu^*-\lambda_n)^2-(U^2/4)][(i\omega_n+\mu^*-\lambda_n)\{1+2G_n\eta_n(X)\}-\eta_n(X)]^2}\ . \quad (28)$$

The derivative of $\eta_n(X)$ with respect to X can be easily determined from the functional form of $\tilde{\chi}_n^0(X)$ in Eq. (21) and the definition of $\eta_n(X)$ in Eq. (24). The derivative of $h(T;X)$ with respect to T is easiest to perform numerically.

The dependence of the transition temperature on X and $|\mu^*|$ is plotted in Figs. 1 and 2 for the case $U/t^*=0.5$ and $U/t^*=2.0$, respectively. The horizontal axis records the label X for the equivalence class of ordered ion configurations and the vertical axis plots the transition temperature at a given value of X. The different curves correspond to different values of the reduced chemical potential $|\mu^*|$. The summations in Eq. (23) are truncated at $N_{\max}=1000$ positive Matsubara frequencies. This truncation provides a lower limit to the numerical determination of transition temperatures. Typically the calculation is accurate for transition temperatures $T_c(X)$ larger than $1/N_{\max}$. The results for $U=0.5$ (Fig. 1) are representative of the weak-coupling regime where the system orders in a chessboard phase for a range of electron concentrations near half filling [$T_c(X)$ has its maximum at $X=-1$]; orders in a series of phases with a continuously varying label $X_{\max}$ for intermediate values of the electron concentration [$T_c(X)$ has its maximum at an intermediate value $-1<X<1$]; and then segregates when the concentration becomes too small or too large [$T_c(X)$ has its maximum at $X=1$]. The transition temperatures for $|\mu^*|=0.5$ are too small to be seen in Fig. 1. The results for $U/t^*=2.0$ (Fig. 2) are indicative of the strong-coupling regime where the system orders in the chessboard phase for concentrations near half filling and then segregates when the concentration becomes too small or too large without passing through any intermediate (long-period) phases [$T_c(X)$ has its maximum only at $X=-1$ or $X=1$]. Note that the transition temperatures for negative values of X tend to be larger than the transition temperatures for positive X.

The label $X_{\max}$ (that determines the equivalence class of the wave vector of the A-ion occupation for the highest-temperature broken-symmetry phase) is determined as a function of U and μ^* by employing both Eq. (23) and Eq. (28) to find the value $X=X_{\max}$ at which $T_c(X)$ is a maximum. An approximation to the zero-temperature phase diagram can now be made with the following assumptions: (a) there are no first-order (discontinuous) phase transitions; (b) the symmetry label $X_{\max}$ of the ordered state does not change as the temperature is lowered from $T_c(X_{\max})$ to 0; and (c) the dependence of the chemical potential μ^* on temperature can be ignored in the range from $T_c(X_{\max})$ to 0. In this case, one assumes the label $X_{\max}$ does not change as $T\to 0$ and determines the electron concentration from Eq. (14) in the zero-temperature limit. At least 5,000 ($N_{\max}=5000$) positive Matsubara frequencies are utilized in the calculation. The electron concentration is restricted to $\rho_e\le\frac{1}{2}$ by using the electron-hole symmetry (4)—the phase diagram for the region $\rho_e\ge\frac{1}{2}$ is determined by rotating the phase diagram for $\rho_e\le\frac{1}{2}$ by 180° about the point $U=0$, $\rho_e=\frac{1}{2}$. The phase diagram is further restricted to $U\ge 0$ by using the A-B interchange symmetry (3)—the phase diagram for the region $U\le 0$ is determined by reflecting the region $U\ge 0$ in a mirror plane along the $U=0$ axis and by applying the conjugation operation to the ion configurations (each configuration Γ with $\rho_i=\frac{1}{2}$ is either self-conjugate $\Gamma^*=\Gamma$ or forms a conjugation pair with another $\rho_i=\frac{1}{2}$ configuration). The value of $X_{\max}$ for the conjugate representation is unchanged.

The critical-phase line where the ordered-phase label changes from positive X to negative X is difficult to determine directly because the transition temperature vanishes at $X=0$. Using the relation $\eta_n'(X=0)=-2\lambda_n^2/G_n$ allows the sign of the derivative of $T_c(X)$ to be determined by evaluating the sign of the numerator of Eq. (28) in the limit $T\rightarrow 0$. The result is expressed as an integral over frequency,

$$\operatorname{sgn}\left.\frac{dT_c(X)}{dX}\right|_{X=0}=\operatorname{sgn}\int_0^\infty d\omega \operatorname{Re}\left\{\frac{G^{-1}(i\omega)[i\omega+\mu-\Sigma(i\omega)-G^{-1}(i\omega)]^2}{[\Sigma(i\omega)+G^{-1}(i\omega)][\Sigma(i\omega)+G^{-1}(i\omega)-(U/2)][\Sigma(i\omega)+G^{-1}(i\omega)-U]}\right\}. \tag{29}$$

The (approximate) zero-temperature phase diagram for the infinite-dimensional case appears in Fig. 3. The horizontal axis measures the interaction strength from weak coupling $[U/(t^*+U)=0]$ to strong coupling $[U/(t^*+U)=1]$. The vertical axis plots the electron concentration ρ_e. The area with left cross hatching is the region of stability for the segregated phase ($X=1$) and the area with right cross hatching is the region of stability for the chessboard phase ($X=-1$). The white region is the area of the phase diagram where $X_{\max}$ varies continuously from 1 to -1. Contour lines of constant $X_{\max}$ (viewed as functions of ρ_e and U) are plotted for $X_{\max}=-0.9$, -0.8, -0.7, -0.6, -0.5, 0.0, and 0.5. Note that the solution of Brandt and Mielsch[12] neglected all of the phase transitions besides the phase transition to the chessboard phase.

The phase diagram in Fig. 3 corresponds closely to physical intuition and previous results for this model.[2,3,6,7] The "Peierls" charge-density-wave distortion requires a finite density of electrons in infinite dimensions before the Fermi-surface effect can open up a large enough gap for a periodic phase to be lower in energy than the segregated phase. The critical concentration is $\rho_e=0.159$, corresponding to a chemical potential of $\mu^*=-1/\sqrt{2}$ [which can be determined by expanding the derivative (at $X=1$) in Eq. (28) for small U and small T]. The chessboard phase is stable for a finite range of electron concentrations near half filling for all finite values of U. The system orders in long-period (possibly incommensurate) phases for intermediate electron concentrations and small interaction strength (weak-coupling regime). This arises from a Fermi-surface effect that opens a gap at the Fermi level for the corresponding electron filling. Finally the system tends toward segregation at large interaction strength because the electron energy is minimized by placing them in the largest possible box in the strong-interaction regime.

It is interesting to note that there is a marked asymmetry between positive and negative values of X for phases labeled by a continuously varying value of X. The negative values of $X_{\max}$ span the range of electron concentrations from $0.22\le\rho_e\le 0.5$ in the limit $U\rightarrow 0$, while positive values of $X_{\max}$ span the much smaller range from $0.16\le\rho_e\le 0.22$ in the same weak-coupling limit. The reason for this asymmetry arises from the fact that the segregated phase is stable for a large range of electron concentrations (due to the significant band filling required for a Peierls-like charge-density-wave distortion in infinite dimensions). The asymmetry between positive and negative values of $X_{\max}$ should decrease as the dimensionality is reduced.

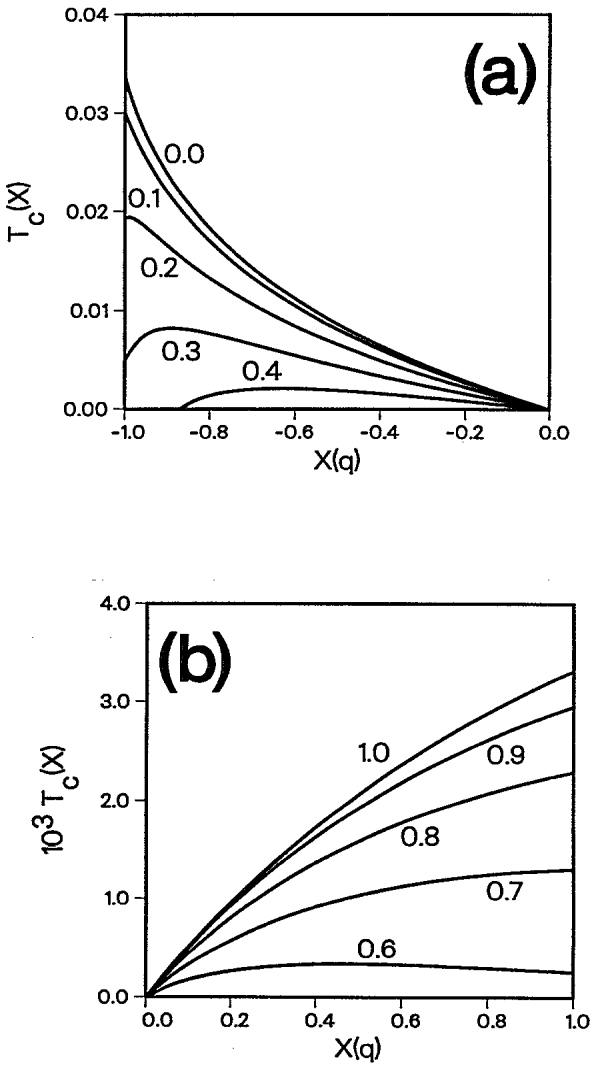

FIG. 1. Transition temperature $T_c(X)$ as a function of wave-vector equivalence class X for the Falicov-Kimball model in $d=\infty$ with $U/t^*=0.5$ (weak-coupling regime). Note that the temperature scales are different for (a) negative and (b) positive values of X. The curves are labeled by the absolute value of the reduced chemical potential $|\mu^*|$. Note that the maximum value of T_c occurs at $X_{\max}=-1$ for small values of the reduced chemical potential $|\mu^*|<0.2$, lies in the range $-1<X_{\max}<0$ for intermediate values $0.2<|\mu^*|<0.5$, lies in the range $0<X_{\max}<1$ for intermediate values $0.5<|\mu^*|<0.7$, and occurs at $X_{\max}=1$ for large values $|\mu^*|>0.7$. Note also that the curves for $|\mu^*|=0.5$ are too small to be seen. The weak-coupling regime orders at intermediate values of X for a range of values of the electron concentration.

The accumulation point for the contours of constant X at $\rho_e=0.312$ ($\mu^*=0.580$) and $U=1.174$ for all negative values of X indicates that the transition temperatures *uniformly* approach zero [$T_c(X)\rightarrow 0$] for all negative values of X in the limit as $\rho_e\rightarrow 0.312$ and $U\rightarrow 1.174$. This phenomenon does not occur for positive values of X.

Recent interest has focused on Fermi-liquid theory for interacting electronic models.[16] The Falicov-Kimball model has a very simple picture of Fermi-liquid theory when put in the language of noninteracting band theory. At fixed interaction strength U, the system orders in a segregated phase for a finite range of electron concentrations, may order in a set of phases labeled by a continuously varying parameter X (weak-coupling regime), and then orders in the two-sublattice chessboard phase. In the region where the ground state is either the segregated phase or the chessboard phase and $0<\rho_e<1/2$ there is no gap at the Fermi level, so the system is a band metal and a Fermi liquid (actually a Fermi gas, since the conduction electrons do not interact among themselves). In the region where the ground state is labeled by the continuously varying parameter X, it is expected that the Fermi level lies in a gap of the band structure producing an insulator that is not a Fermi liquid. These results are similar to those of Ref. 16 where an intermediate range of electron concentrations produced an insulator in a long-range hopping model.

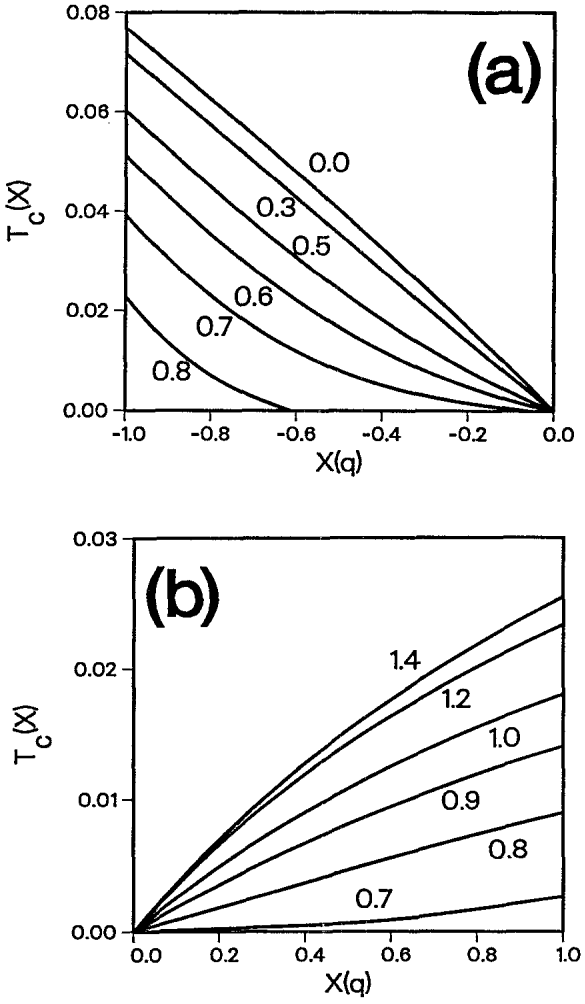

FIG. 2. Transition temperature $T_c(X)$ as a function of wave-vector equivalence class X for the Falicov-Kimball model in $d=\infty$ with $U/t^*=2.0$ (strong-coupling regime). Note that the temperature scales are different for (a) negative and (b) positive values of X. The maximum value of T_c always occurs at $X_{\max}=-1$ for small values of the reduced chemical potential $|\mu^*|<0.85$ and occurs at $X_{\max}=1$ for large values $|\mu^*|>0.85$. The strong-coupling regime never orders at an intermediate value of X for any value of the electron concentration.

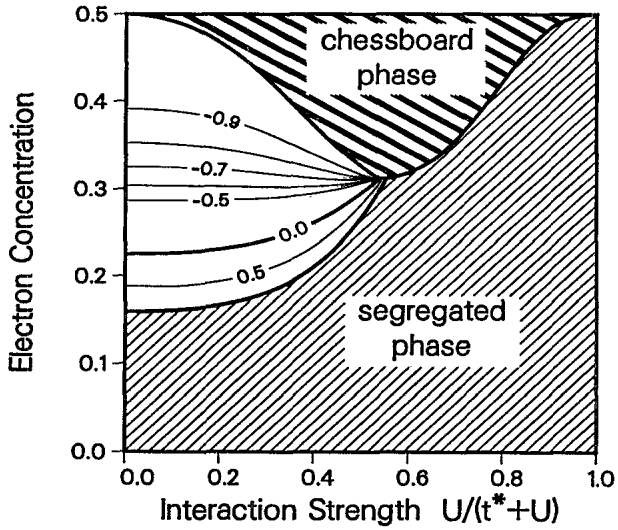

FIG. 3. Phase diagram of the spinless Falicov-Kimball model for the symmetric case in the limit $d=\infty$. The area with left cross hatching is the region of stability for the segregated phase ($X=1$) and the area with right cross hatching is the region of stability for the chessboard phase ($X=-1$). The white region is the area of the phase diagram where $X_{\max}$ varies continuously from 1 to -1. Contour lines of constant $X_{\max}$ are plotted for $X_{\max}=-0.9$, -0.8, -0.7, -0.6, -0.5, 0.0, and 0.5. Note the difference in stability for positive and negative values of X.

IV. THE ONE-DIMENSIONAL CASE

The one-dimensional model does not display any finite-temperature phase transitions. There are, however, numerous level crossings in the ground state as a function of electron concentration and interaction strength. The zero-temperature phase diagram plots the equivalence class of the ground-state configuration as a function of ρ_e and U. There has been recent interest in this model[5,8–10,22,23] and the known results are summarized below.

At small interaction strength the system undergoes a Peierls distortion for all electron fillings with a gap opening up at the Fermi level as the electron concentration is varied. At large interaction strengths the system segregates for all electron concentrations except $\rho_e=\frac{1}{2}$. The chessboard phase appears to be the ground state *only* at $\rho_e=\frac{1}{2}$, and does not possess a finite area of stability in the zero-temperature phase diagram. The system appears to always pass through an intermediate set of (long-period)

ordered phases in the transition from the chessboard phase to the segregated phase. The segregated phase appears to be the only phase that is stable for a finite area of the phase diagram.

It is interesting to test how the results for the infinite-dimensional Falicov-Kimball model compare to the one-dimensional results to see what the effects of dimensionality are on the physics of the model. There is no exact phase diagram for the one-dimensional model that includes all possible (long-period) ordered phases. Instead, there are restricted phase diagrams that approximate the full phase diagram but include only a finite number of periodic phases as candidate ground states for the system. In order to compare these restricted phase diagrams to infinite-dimensional results one needs the analog of the parameter $X(\mathbf{q})$ that played such a crucial role in the infinite-dimensional theory. The simplest analog is to define $X(q)\equiv\cos q_{\max}$, where $q_{\max}$ denotes the wave vector of the maximum Fourier coefficient in the Fourier expansion of the ground-state ion configuration $\Gamma_{gs}=\{W_j\}$. The perturbative analysis of Ref. 5 implies that in the limit $U\rightarrow 0$, $X(q)$ varies from 1 to -1 (as the electron concentration varies from 0 to $\frac{1}{2}$). The mapping $\Gamma\rightarrow X(q)$ remains many to one, since the ground-state ionic configuration Γ_{gs} is determined by more than just its largest Fourier coefficient. The values of $X(q)$ for all of the ionic configurations with periods less than nine are recorded in Table I. The ion configurations Γ are recorded in the alloy language where each lattice site is occupied by an A or B ion. For example, $AABB$ denotes the period-four configuration $\ldots AABBAABB\ldots$ on the linear chain.

The restricted phase diagram of the one-dimensional Falicov-Kimball model (in which the ground states are labeled only by the parameter X) is plotted in Fig. 4. The restricted (incoherent) phase diagram of Ref. 5 is used to construct an approximate zero-temperature phase diagram. The left cross-hatched region corresponds to the area of the phase diagram where the segregated phase

TABLE I. The parameter $X=\cos k_{\max}$ for all of the one-dimensional ion configurations with $\rho_i=\frac{1}{2}$ and periodicity smaller than nine. The wave vector $k_{\max}$ is defined to be the wave vector of the maximum Fourier coefficient of the Fourier transform of the ion configuration $\{W_i\}$. In the case where there is no unique maximum wave vector, the parameter X is determined by averaging over all maximal wave vectors.

Ion	Configuration	X
1	AB	-1
2	$AABB$	0
3	$AAABBB$	$\frac{1}{2}$
4	$AABABB$	$-\frac{1}{2}$
5	$AAAABBBB$	$1/\sqrt{2}$
6	$AAABABBB$	$-\frac{1}{2}$
7	$AAABBABB$	0
8	$AABAABBB$	0
9	$AABABABB$	-1
10	$AABABBAB$	$-1/\sqrt{2}$
11	segregated phase	1

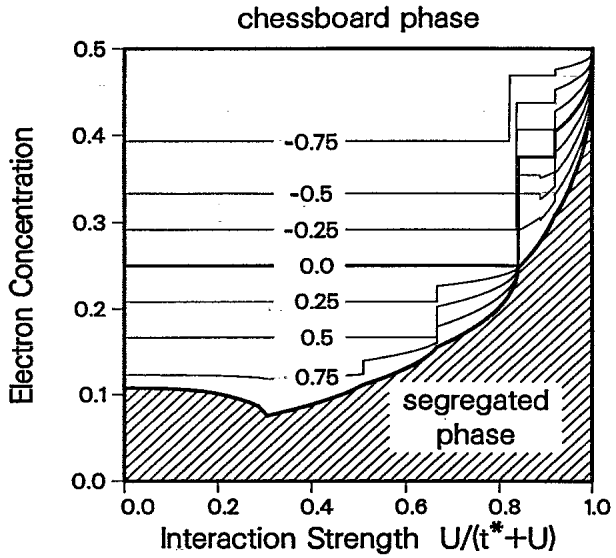

FIG. 4. Approximate phase diagram for the spinless Falicov-Kimball model for the symmetric case in $d=1$ (calculated from the restricted incoherent phase diagrams of Ref. 5). The area with left cross hatching is the region of stability for the segregated phase ($X=1$). The white region is the area of the phase diagram where $X_{\max}$ varies continuously from 1 to -1. Contour lines of constant $X_{\max}$ are plotted for intervals of 0.25 from -1 to 1 (the exact phase diagram is expected to have smooth contour lines of constant X).

($X=1$) is the ground state. The white region contains the area where the label X varies continuously. Contours with a constant value of X are plotted at equally spaced intervals of size 0.25 in the range from 1 to -1. The contours of constant X show discontinuous jumps at the termination points of the coherent phase lines. The constant X contours should become smooth continuous lines and the region where the ground state is labeled by the continuously varying parameter X should extend to $\rho_e=0$ as $U\rightarrow 0$ in the exact phase diagram.

The similarity with the infinite-dimensional phase diagram (Fig. 3) is striking. The label X appears to vary continuously from $X=1$ (segregated phase) to $X=-1$ (chessboard phase) as the electron concentration varies over a range $\rho_c^{\rm seg}(U)\leq\rho_e\leq\frac{1}{2}$. The curvature of the lines of constant X (viewed as a function of U) in the infinite-dimensional model provides a possible explanation for the mysterious "phase islands" present in the one-dimensional model:[5] if the full phase diagram for the one-dimensional model has lines of constant X that are continuous and curved, then one expects phase islands to appear (near the regions where the system segregates) in any restricted (coherent) phase diagram that does not sample at a continuous number of X values.

V. CONCLUSION

The "zero-temperature" phase diagrams for the spinless Falicov-Kimball model (annealed binary alloy) have been reexamined for the limiting cases of large and small

dimensions. The case of a 50%-50% A-B mixture was considered. The results showed that the spinless Falicov-Kimball model is only weakly dependent on the dimensionality of the underlying lattice. Regions of parameter space were identified where the alloy segregates into separate A and B phases, condenses into a two-sublattice periodic arrangement (chessboard phase), and where long-period phases labeled by a continuously varying parameter were favored. This third region of parameter space is quite interesting. It may possess a fractal structure where the periodicity of the ground-state ion configuration is adjusted to match each rational electron concentration.[5,22]

The infinite-dimensional phase diagram separates into two distinct regions. In the weak-coupling regime, the system lies in the segregated phase for a range of electron concentrations from zero up to some finite concentration $\rho_c^{\rm seg}(U)$ that is a function of the interaction strength. As the electron concentration is increased above this critical concentration, the system orders in various long-period (commensurate and incommensurate) phases until the electron concentration is increased to an upper critical concentration $\rho_c^{\rm cb}(U)$ where the system orders into the chessboard phase. The critical concentration for segregation $\rho_c^{\rm seg}(U)$ remains finite in the limit as $U\rightarrow 0$. In the strong-coupling regime these two critical concentrations are equal $[\rho_c^{\rm seg}(U)=\rho_c^{\rm cb}(U)]$ and the system changes directly from the segregated phase to the chessboard phase without any long-period phases intervening. The segregation principle holds, in the sense that the critical concentration approaches $\frac{1}{2}$ as $U\rightarrow\infty$.

The one-dimensional phase diagram is not as well known. It appears to be a singular limit of the infinite-dimensional phase diagram. The one-dimensional model appears to always be in the weak-coupling regime, in the sense that the transition from the segregated phase to the chessboard phase appears to always pass through a region of long-period phases. The one-dimensional model appears to have no finite area of the phase diagram where the chessboard phase is stable; i.e., $\rho_c^{\rm cb}(U)=\frac{1}{2}$ for all U. Finally, the critical concentration for segregation vanishes in the limit of small coupling $[\rho_c^{\rm seg}(U)\rightarrow 0$ as $U\rightarrow 0]$.

It is conjectured that the results for finite dimensions lie in between these two extremes. The finite-dimensional phase diagram will be qualitatively similar to the infinite-dimensional phase diagram, with the following changes: the strong-coupling regime will start at a larger value of U; the area of the phase diagram where the chessboard phase is stable will decrease; and the critical concentration for segregation (in the limit $U\rightarrow 0$) will decrease.

These conjectures can be tested by performing a systematic expansion of the self-energy in orders of $(1/d)$ to calculate the (perturbative) corrections due to finite dimensionality. The simplest (uncontrolled) approximation[18] is to replace the Gaussian noninteracting density of states with the proper density of states for the dimensionality of interest. Further corrections include taking into account the additional (weak) momentum dependence that the self-energy has to order $(1/\sqrt{d})$ (preliminary work along these lines has appeared in Ref. 17). Other cases of interest would include generalizations to examine the model on body-centered-cubic and face-centered-cubic lattices.

The nonsymmetric case $(\rho_i\neq\frac{1}{2})$ is another interesting case to examine. Once again, the segregated phase is expected to dominate the phase diagram. There should be a region where the system is stabilized in long-period phases labeled by the continuous parameter X (the weak-coupling regime). In dimensions larger than one, there is probably a strong-coupling regime where the system changes from a commensurate (short-period) phase directly to the segregated phase.

The solution of the spinless Falicov-Kimball model in infinite-dimensions appears to be the best starting point for understanding the phase diagram of the model in arbitrary dimensions. The phase diagram for the one-dimensional case appears to be a singular limit corresponding to the "weak-coupling" regime of the infinite-dimensional model. The phase diagram for the two- and three-dimensional cases should be qualitatively similar to the infinite-dimensional case incorporating both weak- and strong-coupling regimes. It appears that an expansion in powers of $1/d$, starting from the infinite-dimensional result, will rapidly converge. The success of the large-dimensional limit for understanding the properties of the spinless Falicov-Kimball model suggests that the infinite-dimensional solution and its $1/d$ corrections may be successfully used to understand the physical properties of other interacting models (such as the Hubbard model). Future work on the $1/d$ expansion for the Falicov-Kimball model and other interacting fermionic models will test these conjectures.

ACKNOWLEDGMENTS

The author would like to acknowledge stimulating discussions with D. Belitz, U. Brandt, N. Bulut, D. Cox, A. Georges, V. Janiš, M. Jarrell, D. Johnson, G. Kotliar, C. Myers, and D. Scalapino. This research was supported by the National Science Foundation under Grant Nos. DMR90-02492 and PHY89-04035.

[1]L. M. Falicov and J. C. Kimball, Phys. Rev. Lett. **22**, 997 (1969).

[2]U. Brandt and R. Schmidt, Z. Phys. B **63**, 45 (1986); **67**, 43 (1987).

[3]T. Kennedy and E. H. Lieb, Physica **138A**, 320 (1986); E. H. Lieb, *ibid.* **140A**, 240 (1986).

[4]The critical temperature is zero in one dimension.

[5]J. K. Freericks and L. M. Falicov, Phys. Rev. B **41**, 2163 (1990).

[6]J. Jędrzejewski, J. Lach, and R. Łyżwa, Phys. Lett. A **134**, 319 (1989); Physica **154A**, 529 (1989).

[7]Ch. Gruber, J. Iwański, J. Jędrzejewski, and P. Lemberger,

Phys. Rev. B **41**, 2198 (1990); Ch. Gruber, J. Jędrzejewski, and P. Lemberger, J. Stat. Phys. **66**, 913 (1992).
[8]Ch. Gruber, Helv. Phys. Acta **64**, 668 (1991).
[9]U. Brandt, J. Low Temp. Phys. **84**, 477 (1991).
[10]P. Lemberger, J. Phys. A **25**, 715 (1992).
[11]W. Metzner and D. Vollhardt, Phys. Rev. Lett. **62**, 324 (1989).
[12]U. Brandt and C. Mielsch, Z. Phys. B **75**, 365 (1989); **79**, 295 (1990); **82**, 37 (1991).
[13]P. G. J. van Dongen and D. Vollhardt, Phys. Rev. Lett. **65**, 1663 (1990).
[14]P. G. J. van Dongen, Phys. Rev. B **45**, 2267 (1992).
[15]V. Janiš, Z. Phys. B **83**, 227 (1991).
[16]Q. Si, G. Kotliar, and A. Georges, Phys. Rev. B **46**, 1261 (1992).
[17]R. Vlaming and D. Vollhardt, Phys. Rev. B **45**, 4637 (1992).
[18]A. Georges and G. Kotliar, Phys. Rev. B **45**, 6479 (1992).
[19]J. S. Faulkner, Prog. Mater. Sci. **27**, 1 (1982).
[20]At half filling for the electrons ($\rho_e=\frac{1}{2}$, $\mu^*=0$) the Green's functions are pure imaginary for all frequencies. In this case the critical frequency ω_c is defined by Eq. (13) in the limit as μ^* approaches zero.
[21]P. W. Anderson, Phys. Rev. **109**, 1492 (1958); E. N. Economou and M. H. Cohen, Phys. Rev. B **4**, 396 (1971); E. N. Economou, *Green's Functions in Quantum Physics,* 2nd ed. (Springer-Verlag, Heidelberg, 1983).
[22]M. Barma and V. Subrahmanyam, Phase Trans. **16**, 303 (1989).
[23]R. Łyżwa, Phys. Lett. A **164**, 323 (1992).